Jurnal
Teknologi

Full Paper

PRESSURE DISTRIBUTION ON THE BLADE SURFACE OF AN AUTOMOTIVE MIXED FLOW TURBOCHARGER TURBINE UNDER PULSATING FLOW CONDITIONS

M.H. Padzillah[a*], S. Rajoo[a], R.F. Martinez-Botas[b]

[a]UTM Centre for Low Carbon Transport in cooperation with Imperial College London, Faculty of Mechanical Engineering, Universiti Teknologi Malaysia,81310 UTM Johor Bahru, Malaysia
[b]Department of Mechanical Engineering, Imperial College London, London SW7 2AZ, United Kingdom

Article history
Received
1 January 2016
Received in revised form
18 May 2016
Accepted
15 June 2016

*Corresponding author
mhasbullah@utm.my

Graphical abstract

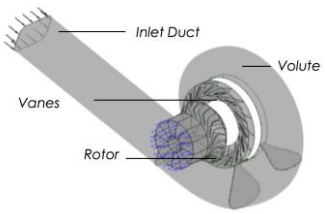

Abstract

The increment of the contribution to CO_2 release by transportation industry as other sectors are decarbonizing is evident. As number of world population continue to increase, the task of developing highly downsized high power-to-weight ratio engines are critical. Over more than a hundred years of invention, turbocharger remains a key technology that enable highly boosted efficient engine. Despite its actual operating environment which is pulsating flow, the turbocharger turbine that is available to date is still designed and assessed under the assumption of steady flow conditions. This is attributable to the lack of understanding on the insight of the flow field effect towards the torque generation of the turbine blade under pulsating flow conditions. This paper presents an effort towards investigating the influence of pulsating flow on the blade loading and its differences from steady state conditions through the use of Computational Fluid Dynamics (CFD). For this purpose, a lean-vaned mixed-flow turbine with rotational speed of 30000 rpm at 20 Hz flow frequency, which represent turbine operation for 3-cylinder 4-stroke engine operating at 800 rpm has been used. Results presented in terms of spanwise location of the blade indicated different behavior at each location. Close to the hub, there are strong flow separation that hinders torque generation is seen while at mid-span more torque is generated under unsteady flow as compared to its steady counterpart. Moreover, close to the shroud, the pressure difference between steady and pulsating flow is almost identical.

Keywords : Mixed-flow turbine, computational fluid dynamics, pulsating flow

Abstrak

Peningkatan kadar pembebasan CO_2 oleh sektor pengangkutan berbanding sektor lain adalah jelas. Oleh kerana bilangan penduduk dunia terus meningkat, adalah sangat penting untuk memastikan engin yang mempunyai nisbah kuasa kepada berat yang tinggi terus dibangunkan. Setalah lebih daripada seratus tahun dicipta, pengecas turbo kekal sebagai teknologi yang penting bagi meningkatkan kecekapan enjin dengan kaedah pemampatan udara. Walaupun pengecas turbo beroperasi dalam keadaan aliran denyutan, namun turbin yang direka bentuk pada masa kini masih lagi berasaskan andaian aliran mantap. Ini adalah disebabkan kekurangan pengetahuan tentang kesan aliran denytan terhadap arah penjanaan tork pada bilah turbin tersebut. Artikel ini membentangkan satu usaha untuk menyiasat pengaruh aliran denyutan terhadap beban yang terhasil pada bilah dan mengkaji perbezaannya dengan aliran mantap melalui keadah Pengiraan Dinamik Bendalir (CFD). Untuk tujuan ini, turbin aliran campuran dengan kelajuan putaran 30000 ppm pada frekuensi aliran 20 Hz, yang mewakili operasi turbin untuk 3-silinder enjin 4 lejang beroperasi pada 800 ppm telah digunakan. Keputusan yang dibentangkan dari segi lokasi arah rentang bilah menunjukkan tingkah laku yang berbeza di setiap lokasi. Berhampiran dengan hab, terdapat pemisahan aliran ketara

telah dilihat dan ini menghalang penghasilan tork. Manakala, pada pertengahan rentang, tork yang lebih tinggi telah dihasilkan oleh aliran denytan berbanding aliran mantap.

Kata kunci: Turbine aliran campuran, dinamik bendalir berbantukan komputer, aliran denyutan

1.0 INTRODUCTION

The continued drive to reduce fuel consumption, and hence CO2 emissions from automotive vehicles are placing ever increasing demands on air charging systems of engines. A widely adopted air charging technology is the turbocharger. Until now, the turbocharger turbine is designed using steady state assumption. The fundamental issue that has not been addressed to date is the mismatch between the reciprocating engine and the turbine. Regardless of the engine operating conditions, the inlet flow to the turbine comprises a highly pulsating flow field with widely varying pressure and mass flow rates, which are not ideal for optimal turbine operation. One of the limiting factors that hinder the development of highly efficient turbocharger turbine that take into advantage the incoming pulsating flow is the lack of understanding of the flow interaction within the turbine stage. In the early days, several experimental attempts have been made to understand the influence of pulsating flow towards the turbine performance. There are conclusive evidences that the turbine performance deviate significantly during pulsating operations when compared to its intended steady flow operations [1][2]. Since then, many attempts to characterize and correlate the turbine behaviour with the properties of incoming pulsating flow. As experimental works involve a certain degree of measurement difficulties, such as to obtain accurate time resolved mass flow rate, it is limited to measurement of the pressure, temperature and torque. The flow feature such as pressure and velocity contour is very difficult to obtained during such works. These difficulties resulted in the numerical simulation of the turbine under pulsating flow conditions.

One of the first researches that attempt to perform Computational Fluid Dynamics (CFD) for pulsating flow is Lam et al.[3]. The objective of this work was to establish the potential use and difficulties of CFD in predicting the turbine performance under such conditions. In simulating the transition between stationary and rotating domain, Lam et al. utilized the Multiple Rotating Frames (MRFs) method. This method is also known as the `frozen rotor' approach, where it is assumed that there are no relative movement between stationary and rotating frames of reference at the time of simulation. The information with regards to rotational speed of the rotor is included in the source terms. One of the issues was the difficulty of getting the simulation to converge properly therefore only qualitative comparisons could be made. Furthermore, the complex geometry of the turbine itself presented a difficulty in defining the exact entry point of unsteady flow at the rotor inlet. Despite that, the work of Lam proved that it was possible to further understand the complexity of pulsating flow by means of full 3-D CFD.

Palfreyman and Martinez-Botas [4] improved the CFD work on pulsating flow by utilizing 'sliding-plane' interface between stationary and rotating domain. They indicated that the method leads to more accurate prediction and proved it by extensive validation procedure with the work of Karamanis [5]. Palfreyman and Martniez-Botas indicated that the tor flow field in the turbine passage under pulsating flow condition is highly disturbed. They also shown that the effect of blades passing the volute tongue effect the flow mostly in the inducer region. The poor flow guidance at the turbine inlet and exit has also been observed and attributed to the assumption of quasi-steady conditions during the design stage of the turbine.

Another work that extensively used CFD approach to simulate flow field behaviour is conducted by Hellstrom and Fuchs [6]. They varied the inlet condition of the turbine volute by introducing disturbances such as turbulence and swirls to see their effect on the turbine performance. Hellstrom and Fuchs indicated that turbulence and swirls effect the flow by introducing additional pressure loss and unfavourable radial velocity distribution respectively. These ultimately result in the reduction of power generation capability of the turbine. Despite successful simulation procedures with high number of node counts, the work of Hellstrom and Fuchs was not validated experimentally.

Recent work by Copeland et al. [7] utilized CFD approach in an attempt to characterize the level of 'unsteadiness' within the turbocharger turbine stage. This is done by defining a new parameter called 'lambda parameter' that represents the ratio of the time-averaged rate of change of the mass flow within the domain to the time-averaged of the through flow mass. This work indicated that the rotor stage is not wholly quasi-steady but is insignificant enough as compared to the volute stage. Building on the work of Copeland, Newton [8] indicated that the overall entropy generation in the pulsating case was 1.66% higher than the corresponding steady state condition, and could be attributed primarily to an increase in entropy generation in the nozzle-rotor interspace region.

The work presented in this paper aims to provide readers on the flow field effect on the pressure distribution on the blade surface. It compares the pressure behaviour between steady and pulsating flow at different span of the blade.

2.0 METHODOLOGY

2.1 Experimental Methodology

Figure1 shows the schematics of the cold-flow turbocharger test facility used in this research located at Imperial College London. This facility, which is originally developed by Dale and Watson [1] is fully equipped to be used for both steady and pulsating flow testing. The compressed air for the test rig is supplied by three screw-type compressors with capacity up to 1 kg/s at maximum absolute pressure of 5 bars. Before the air flow is channelled into two 81.40mm limbs, it is pre-heated to 345 K to prevent condensation during air expansion in the turbine. The two limbs enable testing not only for single entry turbine but also for multiple entry turbine. The mass flow rate in both limbs is measured using both the electronic v-cone flowmeter as well as the orifice plates. Downstream the orifice plates is a specially cut-out pulse generator originally designed by Dale and Watson in 1986. The pulse generator allows for replication of the actual pressure pulse in the exhaust manifold. It is capable of generating pulses up to 80 Hz. For the steady flow testing, the pulse generator is defaulted to 'fully open' position to allow maximum steady-state flow area. Downstream the pulse generator is the 'measurement plane' that consist of a few measurement devices. This includes instantaneous pressure sensors, hotwire anemometer and thermocouples.

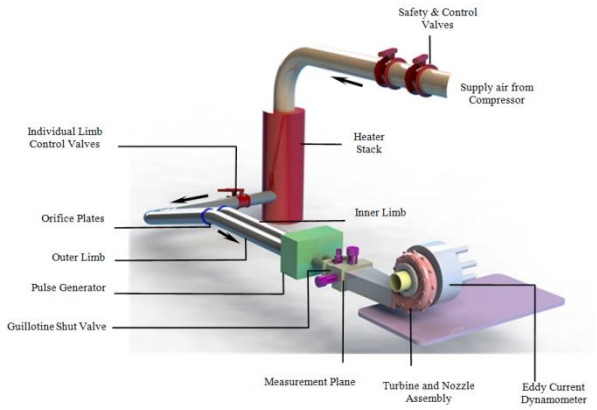

Figure 1 Imperial College 'cold flow' turbocharger test facility

The turbine is attached to a 60kW eddy current dynamometer originally developed by Szymko [9]. The reaction force on the dynamometer assembly is measured by a 20kg load cell on the gimbal-mounted dynamometer housing. The heat that is released by the dynamometer stator is heavily cooled by a water cooling system. The temperature of the stator plate is constantly monitored and electronically linked to the mainframe for automatic shut-down in case of overheating. The dynamometer also places an optical sensor for the purpose of instantaneous speed measurement.

2.2 Numerical Methodology

The numerical works conducted in the current research utilized a commercial CFD software Ansys CFX 14.1. There are in total of 4 main components involved in building the solid model of the turbocharger turbine geometry. These components are known as a 40mm chord length mixed flow turbine, 15 stationary vanes, a modified Holset H3B volute[10] and also the inlet duct. The constructions of these individual components differ accordingly. The components that are directly related with rotordynamics such as the rotor and vanes are created in TurboGrid. This is done by specifying profile lines that contains Cartesian coordinates of hub, shroud and blade. 3 profile lines were specified in the construction of the nozzle blade. Meanwhile, due to its geometrical complexity, 8 profile lines are specified in the construction of the rotor. These lines were generated earlier using Bezier polynomial with the control points specified by Abidat [11] in 1991 to suit high loading turbine operation. Figure 2(a) shows the resultant polynomial lines that forms hub (blue line) and shroud (red line) of the rotor wheel. The dotted line in Figure 2(a) indicated the imaginary position of the leading and trailing edge of the rotor. It can be seen that the overall chord length is 40 mm. Figure 2(b) shows the curvature for leading edge and camber line of the blade. Meanwhile, the constructions of general components such as inlet duct and turbine volute were done using Solidworks. These solid models are then transferred into meshgeneration software ICEM CFD. This software allows for specification of hexahedral mesh throughout the whole geometry. The components that are meshed using turbogrid are structured hexahedral mesh wherears the ones that are generated using ICEM CFD are unstructured hexahedral mesh. The total number of nodes in the assembly is 4.5 millions.

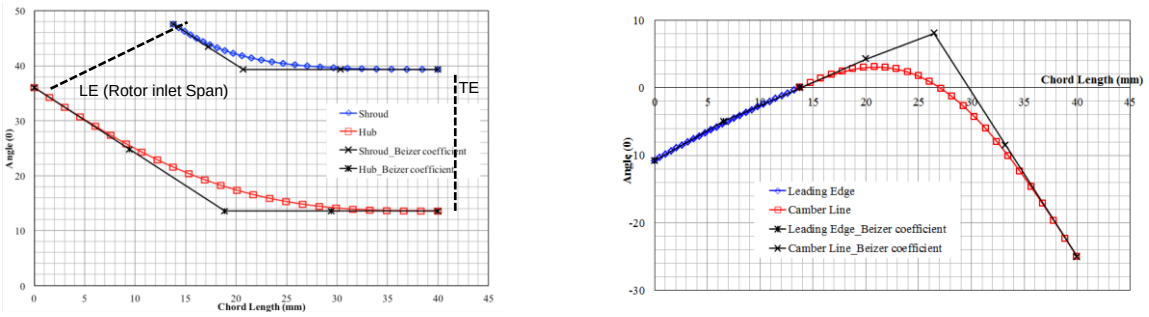

(a) (b)

Figure 2 Development of turbine geometry using Bezier Polynomial

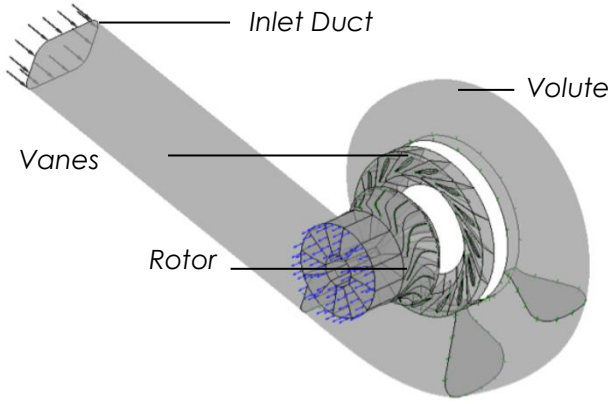

Figure 3 Assembly of domain in CFX-Pre

After the meshing process of each of the components is completed, they we assembled to form a complete domain in Ansys CFX-Pre. This process is shown in Figure 3. For the specification of interface, the connections between stationary parts are defined as general connection. Meanwhile, the connecting surface between rotor (rotating) and stationary vanes is defined as the transient-rotor stator interface. This allows for relative movement between rotor and stator thus resulted in more accurate flow prediction.

The boundary conditions at inlet require the specification of either mass flow rate or total pressure. For current work, the time varying total pressure and temperature are set at this particular inlet location. The inlet parameters are area averaged at the inlet surface so that it only changes temporally. The values of these parameters were obtained at the measurement plane earlier during the experimental procedure. The direction of inlet flow is defined so that the only velocity component that exists is normal to the inlet plane. At the outlet boundary, static atmospheric pressure is specified. At the walls, no-slip boundary condition is set. This includes the wall of vanes and rotor blades. Due to the availability of experimental data at 30000rpm rotor rotation (equivalent to 50% design speed), it is decided that this speed are to be used to enable directcomparison with existing data

3.0 RESULTS AND DISCUSSION

3.1 Validation Procedure

Before the analysis is conducted, the computed models are validated with experimental results. This procedure is done by computing the turbine performance parameters which are the turbine efficiency, velocity ratio, mass flow parameter (also known as swallowing capacity) and pressure ratio from CFD results and comparing them with actual experimental data.

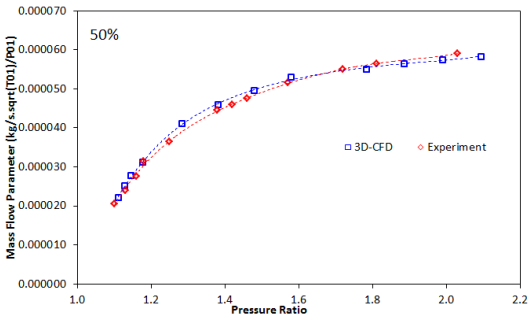

(a)

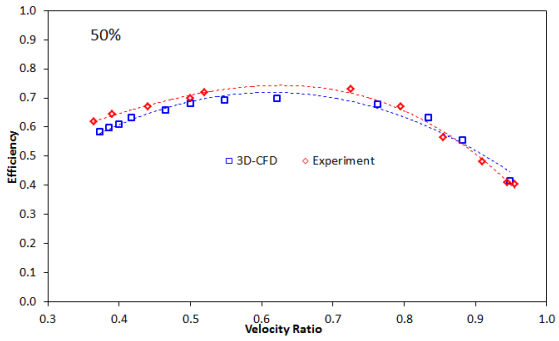

(b)

Figure 4 Comparison between CFD and Experimental data of (a) Mass Flow Parameter vs Pressure Ratio and (b) Efficiency vs Velocity Ratio

The plot of comparison between mass flow parameter against pressure ratio for CFD and experimental data is shown in Figure 4(a). Figure 4(a) indicated that the developed numerical model is able to capture both trend and magnitude of the turbocharger turbine mas flow parameter sufficiently well throughout the range of operation. The calculated Root Mean Square of the deviation is recorded to be 2%.

Meanwhile, the comparison process between CFD and experimental data for efficiency is relatively more challenging than that of mass flow parameter. This is due to its dependency of multiple parameters such as mass flow rate, total temperature, torque and also pressure. Any deviation on these parameters would enhance the differences of the calculated and measured efficiency values. The application of constants such as the specific heat value could also potentially effect accuracy of the prediction. The comparison between CFD and experimental data of the efficiency plot is shown in Figure 4(b). In this plot, it can be observed that CFD recorded under prediction of the efficiency value at velocity ratio 0.85 and below. This deviation achieved its maximum value at 0.36 velocity ratio where the predicted efficiency is 5 points higher than experimentally measured value. The overall deviation indicated by Root Mean Square value is 2 efficiency points. In general, despite recorded deviations, the prediction points are well below the experimental uncertainty limits and as such is sufficiently accurate for the flow field analysis.

3.2 Analysis of pressure on the blade surfaces

This section intends to discover the power generation capability at particular locations of the turbine blades at different operating conditions. The torque produced by the blade depends on the pressure difference between the pressure and suction surface of the blade. In order to visualize the details of the pressure distribution at on the blade surface, the normalized pressure are plotted for a few spanwise planes for all four conditions of interest. Three spanwise planes at 5%, 50% and 95% spanwise location are selected and the positions of these planes are visualized in Figure 5. Figure 6 shows the instances that the analysis is focused on. Pt1 and pt2 is the instances at similar level of pressure during pressure increment and decrement period respectively. Pt4 also has similar pressure level but the turbine is operating under steady state condition. Meanwhile, pt3 indicated maximum pressure at the particular operation frequency.

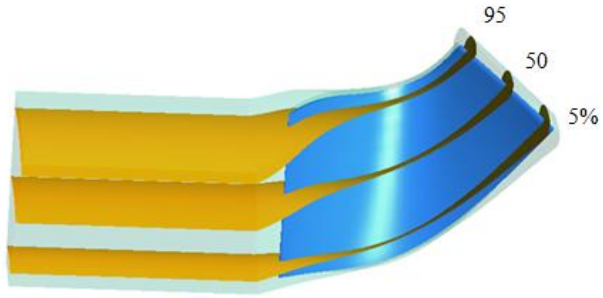

Figure 5 Orientation of blade-to-blade planes

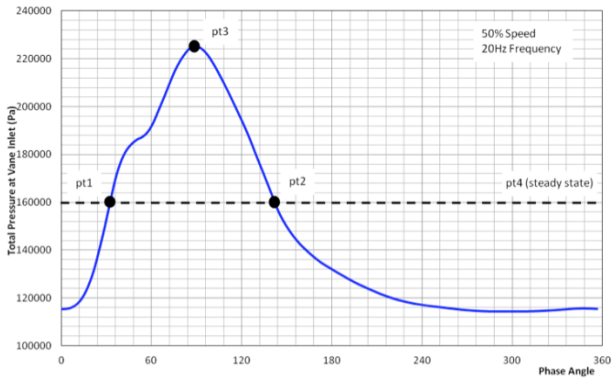

Figure 6 Steady and unsteady operating condition for flow field analysis

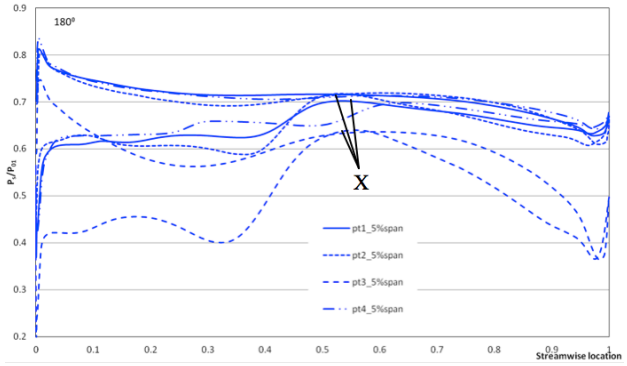

(a)

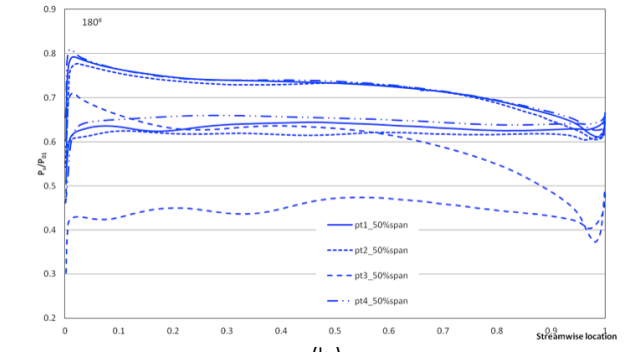

(b)

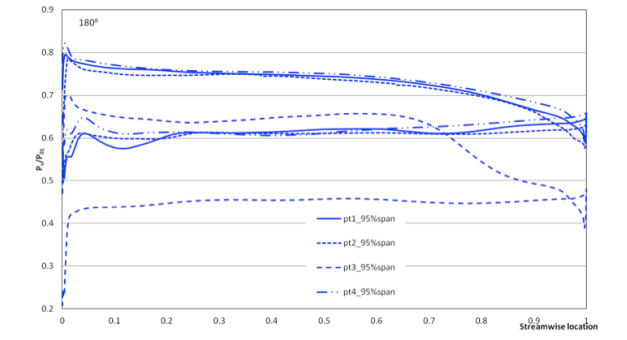

(c)

Figure 7 Plot of normalized surface pressure of the blade at (a) 5% span, (b) 50% span and (c) 95% span

Figure 7 shows the plot of normalized static pressure at different span of the blade surface for different operating conditions. Streamwise position 0.0 indicated leading edge while position 1.0 indicated the blade trailing edge.Figure 7reveals that the most distorted pressure loading occur close to the hub region (Figure 7(a))where multiple flow separations (indicated by sudden increase in P_5/P_{01} value) are detected as the flow travels the entire streamwise length. For current conditions where the relative flow angle is positive, the flow separation is likely to occur on the suction surface than the pressure surface. During pulsating flow turbine operations (pt1, pt2 and pt3), close to the hub region, the pressure difference between pressure and suction surface (therefore the blade power generation capability), is reduced to almost negligible value, even slightly negative value (work is transferred from the rotor blade to the fluid) between 50% to 60% streamwise location. This feature is indicated by label X inFigure 7. Meanwhile, for pt4 (steady-state condition), even though the separation region is still visible, the entire streamwise length of the blade is shows higher pressure level on the pressure surface than the suction surface (positive torque).

At 50% spanwise location (Figure 7(b)), it is interesting to see that pt1, pt2, and pt4 have almost similar pressure profile at the pressure surface. On the other hand, at the suction surface, pt1 and pt2 have lower pressure distribution at all locations as compared to pt4. This observation suggests that at similar inlet total pressure, turbine operating under pulsating flow condition is capable of generating more power at mid-span of the blade as compared to its steady counterpart. Moreover, the power generated when the pressure is decreasing in a pulse (pt2) is higher at the blade mid-span as compared to the instance where the pressure is increasing (pt1). Meanwhile, at the highest pressure instance in a pulse (pt3), the pressure difference between pressure and suction surface is constantly higher than the other conditions throughout the entire streamwise locations.

The surface pressure distribution recorded at 95% spanwise location (close to the shroud) shows slightly different behaviour compared to mid-span location (as shown in Figure 7(c)). It can be seen in Figure 7(c) that the pressure difference is higher for all pt1, pt2 and pt4 at 95% span then at 50% span. Furthermore, their magnitudes are now almost similar where no clear differences can be seen except close to the leading and trailing edge of the blade. Therefore, this behaviour indicates that at this particular spanwise location, neither steady nor pulsating flow have the advantage in terms of the power generation capability. The other feature indicated in Figure 7(c) is that the surface pressure difference for pt3 drops very quickly downstream of the 70% streamwise location.

These analyses have yielded several interesting observations. The observation indicated that the most distorted pressure distribution on the blade surface occur at the suction surface close to the rotor hub. Multiple flow separations that reduce the power generation capability at this region have been

detected. Moreover, the turbine shows the capability of generating more power at mid-span of the rotor blade during pulsating flow operation as compared to its steady counterpart. However, close to the shroud, neither steady nor pulsating flow operations have the advantage in terms of the power generation capability.

4.0 CONCLUSION

In this research, full 3D computational models under pulsating flow operating conditions have been developed. The CFD results have been validated with experimental data, thus ensuring validity of the model. The analyses on this work look at the pressure distribution on the surface of the rotor blade. It has been found that the flow suffers multiple separations close to the rotor hub regardless of its operating conditions. Small torque generation due to insufficient pressure difference between the pressure and suction surface of the blade is seen close to the rotor hub under pulsating flow conditions. Further observation also indicated that the power generation of the blade at mid-span is greater during pulsating flow conditions than steady flow conditions. Finally, close to the shroud, both steady and pulsating flow operations indicated almost similar amount of torque generation.

Acknowledgement

The corresponding author would like to acknowledge Universiti Teknologi Malaysia (VOT number: Q.J130000.2624.11J22) for the financial support on this research.

References

[1] A. Dale and N. Watson. 1986. Vaneless Radial Turbocharger Turbine Performance, *Proc. IMechE Int. Conf. Turbocharging Turbochargers (Mechanical Eng. Publ. London)*. 65–76.

[2] S. S. Shamsi. 1979. Estimating the Influence of Pulsating Flow Conditions on the Performance of a Turbine. *SAE Technical Paper 790068*

[3] J. .-W. Lam, Q. D. H. Roberts, and G. T. McDonnel. 2002. Flow Modelling of a Turbocharger Turbine Under Pulsating Plow, *Preceedings IMechE Int. Conf. Turbochargers Turbochargnig*.181–197.

[4] D. Palfreyman and R. F. Martinez-Botas. 2004. The Pulsating Flow Field in a Mixed Flow Turbocharger Turbine: An Experimental and Computational Study. *Proceedings of the ASME Turbo Expo 2004*. 5:697–708.

[5] D. Palfreyman and R. Martinez-Botas, 2002, Numerical Study of the Internal Flow Field Characteristics in Mixed Flow Turbines, *Proc ASME Turbo Expo No. GT2002-30372*.

[6] N. Karamanis, R. F. Martinez-Botas, and C. C. Su. 2001. Mixed Flow Turbines: Inlet and Exit Flow Under Steady and Pulsating Conditions. *Journal of Turbomachines.* 123(2): 359.

[7] N. Karamanis, D. Palfreyman, C. Arcoumanis, and R. F. Martinez-Botas. 2006. Steady and Unsteady Velocity Measurements in a Small Turbocharger Turbine with Computational Validation. *Journal of Physics Conference Series.* 45(1):173.

[8] M. H. Padzillah, S. Rajoo, and R. F. Martinez-Botas. 2015. Phase Shift Methodology Assessment of an Automotive Mixed Flow Turbocharger Turbine Under Pulsating Flow Conditions. *Jurnal Teknologi*. 77(8):29–35.

[9] M. H. Padzillah, S. Rajoo, and R. F. Martinez-Botas, 2015, Experimental and Numerical Investigation on Flow Angle Characteristics of an Automotive Mixed Flow Turbocharger Turbine. *Jurnal Teknologi.* 77(8):7–12.

[10] M. H. Padzillah, S. Rajoo, and R. F. Martinez-Botas. 2015. Flow Field Analysis of an Automotive Mixed Flow Turbocharger Turbine. *Jurnal Teknologi*. 77(8):21–27.

[11] F. Hellstrom and L. Fuchs. 2008. Effects of Inlet Conditions on the Turbine Performance of a Radial Turbine. *Volume 6: Turbomachinery, Parts A, B, and C*. 6:1985–2001.

[12] C. D. Copeland, R. Martinez-Botas, M. Seiler, and N. P. 2010. The Effect of Unequal Admission on the Performance and Loss Generation in a Double-Entry Turbocharger Turbine. *Proc ASME Turbo Expo No. GT2010-22212*.

[13] C. D. Copeland, P. Newton, R. F. Martinez-Botas, and M. Seiler. 2012. A Comparison of Timescales Within a Pulsed Flow Turbocharger Turbine.*10th International Conference on Turbochargers and Turbocharging*. 389–404.

[14] P. Newton, R. Martinez-Botas, and M. Seiler. 2014. A Three-Dimensional Computational Study of Pulsating Flow Inside a Double Entry Turbine. *J. Turbomach.*137(3): 031001.

[15] S. Szymko. 2006. The Development of an Eddy Current Dynamometer for Evaluation of Steady and Pulsating Turbocharger Turbine Performance. Imperial College of Science, Technology and Medicine, University of London.

[16] S. Rajoo and R. Martinez-Botas. 2006. Experimental Study on the Performance of a Variable Geometry Mixed Flow Turbine for Automotive Turbocharger. *8th International Conference on Turbochargers and Turbocharging*. 183–192.

[17] M. Abidat. 1991. Design and Testing of a Highly Loaded Mixed Flow Turbine. Imperial College of Science, Technology and Medicine, University of London.

.